Journal Pre-proof

Protective role of cinnabar and realgar in Hua-Feng-Dan against LPS plus rotenone-induced neurotoxicity and disturbance of gut microbiota in rats

Ce Chen, Bin-Bin Zhang, An-Ling Hu, Huan Li, Jie Liu, Feng Zhang

PII: S0378-8741(19)31429-1

DOI: https://doi.org/10.1016/j.jep.2019.112299

Reference: JEP 112299

To appear in: *Journal of Ethnopharmacology*

Received Date: 9 April 2019

Revised Date: 11 September 2019

Accepted Date: 9 October 2019

Please cite this article as: Chen, C., Zhang, B.-B., Hu, A.-L., Li, H., Liu, J., Zhang, F., Protective role of cinnabar and realgar in Hua-Feng-Dan against LPS plus rotenone-induced neurotoxicity and disturbance of gut microbiota in rats, *Journal of Ethnopharmacology* (2019), doi: https://doi.org/10.1016/j.jep.2019.112299.

This is a PDF file of an article that has undergone enhancements after acceptance, such as the addition of a cover page and metadata, and formatting for readability, but it is not yet the definitive version of record. This version will undergo additional copyediting, typesetting and review before it is published in its final form, but we are providing this version to give early visibility of the article. Please note that, during the production process, errors may be discovered which could affect the content, and all legal disclaimers that apply to the journal pertain.

© 2019 Published by Elsevier B.V.

Graphical abstract

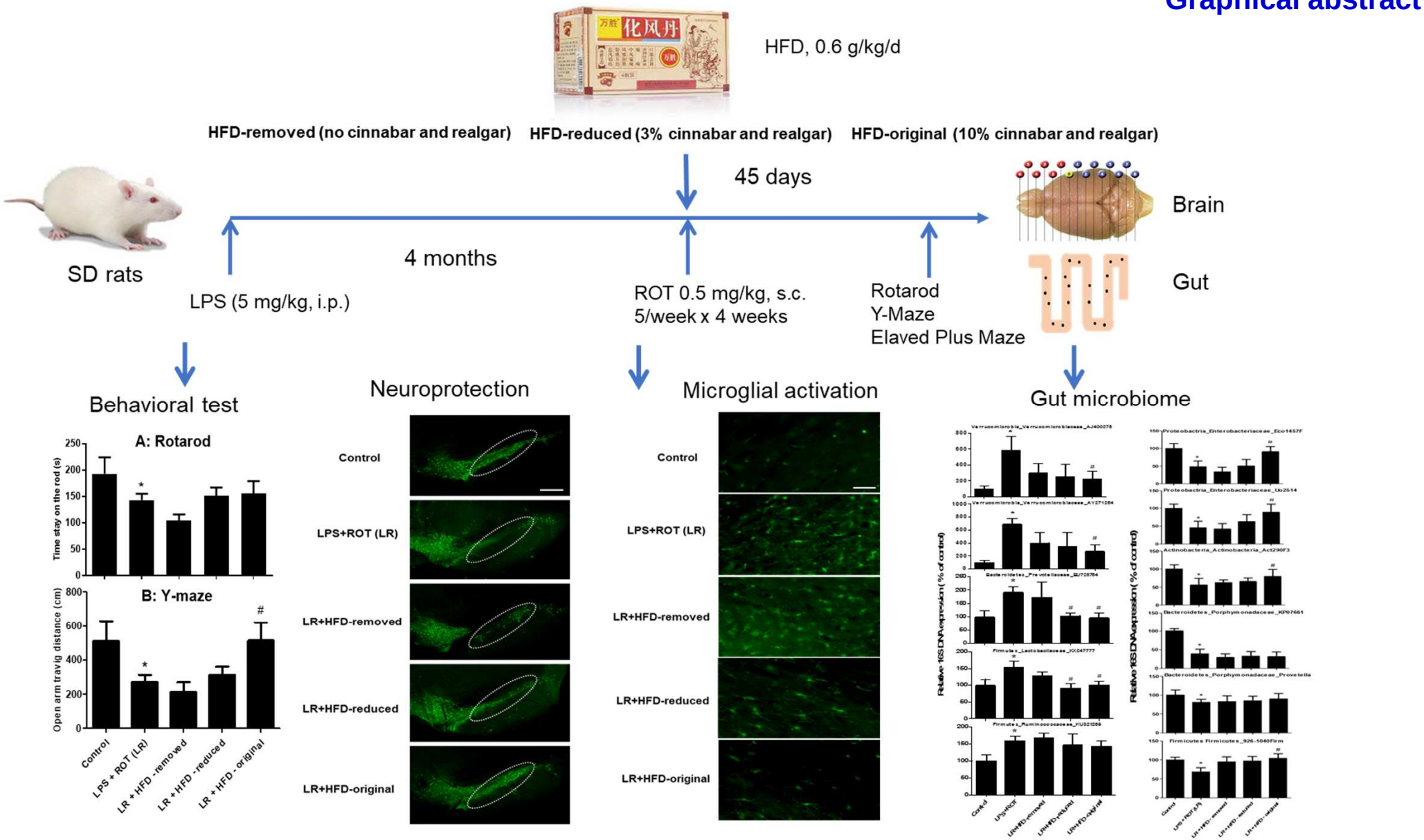

Journal Pre-proof

Title page

Title: Protective role of cinnabar and realgar in Hua-Feng-Dan against LPS plus rotenone-induced neurotoxicity and disturbance of gut microbiota in rats

Authors:

Ce Chen, Bin-Bin Zhang, An-Ling Hu, Huan Li, Jie Liu*, Feng Zhang*

Key Laboratory of Basic Pharmacology of Ministry of Education and Joint International Research Laboratory of Ethnomedicine of Ministry of Education, Zunyi Medical University, Zunyi, Guizhou, China

***Correspondence:** Feng Zhang, email: zhangfengzmc@163.com, Jie Liu, email: Jie@liuonline.com

Running title: Role of cinnabar and realgar in Hua-Feng-Dan neuroprotection

Abbreviations: HFD, Hua-Feng-Dan; LPS, lipopolysaccharide; ROT, rotenone; THir, Tyrosine hydroxylase immune-reactive; IBA-1, ionized calcium binding adapter molecule 1

Journal Pre-proof

Highlights

- Hua-Feng-Dan (HFD) protected rats from LPS plus Rotenone-induced dopamine neuronal loss and behavioral dysfunction
- HFD ameliorated LPS plus Rotenone-induced microglial activation
- HFD attenuated LPS plus Rotenone-induced disruption of gut microbiome
- Cinnabar and realgar were the active ingredients in HFD to exert beneficial effects

Journal Pre-proof

Abstract

Ethnopharmacological relevance: Hua-Feng-Dan (HFD) is a traditional Chinese medicine used for neurological disorders. HFD contains cinnabar (HgS) and realgar (As_4S_4). The ethnopharmacological basis of cinnabar and realgar in HFD is not known.

Aim of the study: To address the role of cinnabar and realgar in HFD-produced neuroprotection against neurodegenerative diseases and disturbance of gut microbiota.

Materials and methods: Lipopolysaccharide (LPS) plus rotenone (ROT)-elicited rat dopaminergic (DA) neuronal damage loss was performed as a Parkinson's disease animal model. Rats were given a single injection of LPS. Four months later, rats were challenged with the threshold dose of ROT. The clinical dose of HFD was administered via feed, starting from ROT administration for 46 days. Behavioral dysfunction was detected by rotarod and Y-maze tests. DA neuron loss and microglial activation were assessed via immunohistochemical staining and western bolt analysis. The colon content was collected to extract bacterial DNA followed by real-time PCR analysis with 16S rRNA primers.

Results: LPS plus ROT induced neurotoxicity, as evidenced by DA neuron loss in substantia nigra, impaired behavioral functions and increased microglial activation. HFD-original (containing 10% cinnabar and 10% realgar) rescued loss of DA neurons, improved behavioral dysfunction and attenuated microglial activation. Compared with HFD-original, HFD-reduced (3% cinnabar and 3% realgar) was also effective, but to be a less extent, while HFD-removed (without cinnabar and realgar) was ineffective. In analysis of gut microbiome, the increased *Verrucomicrobiaceae* and *Lactobacteriaceae*, and the decreased *Enterobacteeriaceae* by LPS plus ROT were ameliorated by HFD-original, and to be the less extent by HFD-reduced.

Conclusion: Cinnabar and realgar are active ingredients in HFD to exert

beneficial effects in a neurodegenerative model and gut microbiota.

Keywords: Hua-Feng-Dan (HFD); cinnabar; realgar; dopaminergic neuron; neurotoxicity; gut microbiome

Journal Pre-proof

Journal Pre-proof

1. Introduction

Hua-Feng-Dan (HFD) is a traditional Chinese medicine that has been used for the treatment of neurological disorders, such as stroke and Parkinson's disease (PD) for 300 years (Zhang et al., 2012). The original HFD recipe contains 10% cinnabar (96% as HgS) and 10% realgar (90% as As_4S_4), along with other components, such as Jingjie (*Nepeta cataria*), Tianma (*Gastrodia elata*), Jiangchan (*Bombyx batryticatus*), Tiannanxing (*Arisaema erubescens*) , Baifuzi (*Aconitum coreanum*), Cangshu (*Atractylodes japonica*) and Quanxie (*Buthus martensii Karsch*) (Liu et al., 2018; Liu et al., 2008a; Zhang et al., 2012). Mercury (Hg) and arsenic (As) are known toxic metal/metalloids (Liu et al., 2008b). In complying with Chinese regulations (Pharmacopoeia et al., 2015; Zhou et al., 2009), the amounts of cinnabar and realgar were reduced from 10% to 3%, resulting in the reduced efficacy (Zhang et al., 2012). Are cinnabar and realgar essential to its therapeutic effects? Our previous studies indicated that cinnabar and realgar were confirmed to be the main active components of HFD *in vitro* (Zhang et al., 2012; Zhang et al., 2010). However, the role of cinnabar and realgar in HFD-mediated neuroprotection *in vivo* was not illuminated.

Several lines of evidence demonstrated that gut microbiome affected brain health in various ways. Bacterial components, such as LPS, conferred low-grade tonic stimulation of the innate immune system. Excessive stimulation from bacterial dysbiosis, small intestinal bacterial overgrowth and increased intestinal permeability might generate systemic brain inflammation. In addition, bacterial enzymes could produce neurotoxic metabolites, such as D-lactic acid and ammonia, to further induce neurotoxicity. Thus, central nervous system effects of the gut microbiome might be produced by immunologic, biochemical, or neuroendocrine mechanisms (Galland et al., 2014). Recently, the emerging reports about microglia-gut connections imply the importance of brain-gut-microbiota in neurodegenerative diseases (Martin

et al., 2018; Perezpardo et al., 2018; Wang et al., 2018). ROT is confirmed to alter gut microbiota (Lai et al., 2018; Perezpardo et al., 2018; Sun et al., 2018). Unhealth gut leads to unhealth brain, and gut microbiota are now recognized as one of the major causes of neurodegenerative disorders (Spielman et al., 2018). Intestinal bacterial dysbiosis might play an important role in the disruption of intestinal epithelial integrity and intestinal inflammation, leading to α-synuclein aggregation and PD pathology (Dodiya et al., 2018).

To address the role of cinnabar and realgar in HFD-produced neuroprotection against neurodegenerative diseases, chronic lipopolysaccharide (LPS) plus rotenone (ROT)-induced rat dopaminergic (DA) neuronal damage as a PD animal model to examine the neuroprotective effects of HFD-original (containing 10% cinnabar and 10% realgar), HFD-reduced (containing 3% cinnabar and 3% realgar), and HFD-removed (without cinnabar and realgar). Their effects on gut microbiome were also examined in the association with neuroprotective effects.

2. Materials and Methods

2.1 Reagents

LPS (Escherichia coli serotype 0111:B4; L4130) and ROT were purchased from Sigma (St. Louis, MO, USA). HFD-original (containing 10% cinnabar and 10% realgar), HFD-reduced (3% cinnabar and 3% realgar) and HFD-removed (without cinnabar and realgar) were provided by Guizhou Wansheng Pharmaceutical Co. (Guizhou, China). Polyclonal mouse anti-Tyrosine Hydroxylase (TH) antibody was from Abcam (Cambridge, MA, USA). Polyclonal rabbit anti ionized calcium binding adapter molecule 1 (IBA-1) antibody was purchased from Proteintech Group (Chicago, IL, USA). TIANamp Stool DNA Kit was bought from Tiangen Biotechnology Company (Beijing, China). All other chemicals were of reagent grade.

2.2 Animals and treatment

Eight-week male (160-180 g) Sprague-Dawley (SD) rats were purchased from the Experimental Animal Center of the Third Military Medical University (Chongqing, China; Certificate No. SCXK 2012-0011). Rats were fed rodent chow in the SPF-grade animal facilities with 21 ± 2°C and the light on from 8:00 to 20:00 at Zunyi Medical University. All animal experiments were performed in accordance with Chinese Guidelines of Animal Care and Welfare and approved by the Animal Care and Use Committee of Zunyi Medical University (2015-07). Rats were acclimated for one week and received a single injection of LPS (5 mg/kg, i.p.). Four months later, rats were challenged with the threshold dose of ROT (0.5 mg/kg in 2% DMSO corn oil, s.c., 5 times/week for consecutive 4 weeks) (Qin et al., 2007; Qin et al., 2013; Radad et al., 2013). Starting from ROT treatment, rats were given standard rodent chow (Normal control and LPS plus ROT (LR) model) or specifically prepared feed (smashed the rodent chow to the powder, mixed with HFD, and 60°C overnight to dry) and designated as LR+HFD-removed (without cinnabar and realgar); LR+HFD-reduced (containing 3% cinnabar and 3% realgar), and LR+HFD-original (containing 10% cinnabar and 10% realgar). The dose selection of HFD was based on the clinical dose. After rat/human dose conversion (approximately 10-fold), the dose of HFD was approximately 0.6 g/kg/d (Taking the assumption of 100 g/kg feed/day, i.e., 6 g HFD/kg feed) and the doses of cinnabar and realgar in HFD-original and HFD-reduced were 0.06 g/kg/d and 0.018 g/kg/d, respectively. Rats were given the drug-containing feed for 45 days. The indexes were detected as shown in **Figure 1**.

2.3 Immunohistochemical staining

DA neurons were recognized with an anti-TH antibody and microglia with IBA-1. Briefly, under anesthesia, rats were transcardially perfused with 4% formaldehyde. Then, brains were removed and post fixed in 4% formaldehyde

for 48 h, followed by 30% sucrose at 4°C until the brains sunk. The brains were cut into 35-μm sections on a horizontal sliding microtome. A total of 36 consecutive brain slices through the entire Substantia nigra (SN) were collected for immunocytochemical staining by every 6 sections. The free-floating sections were first treated with 0.3% Triton X-100 for 30 min, and immune-blocked with 4% goat serum in 0.25% triton/PBS for 2 h and then incubated with anti-TH antibody (1:1000) and anti-IBA1 antibody (1:1000) overnight at 4 °C. After washing, brain slices were incubated with Alexa-488 (green) conjugated secondary antibodies (1:1,000) for 1 h to visualize the TH positive cells. An Olympus microscope (Olympus, Tokyo, Japan) was used to collect the digital images of SN TH positive neurons and IBA-1 positive microglia. The number of TH positive cells and IBA-1 positive cells were counted (Li et al., 2019).

2.4 Western blot analysis

The total protein was extracted from the midbrain tissues and the protein concentration was measured with the BCA protein assay kit (Beijing Solarbio Science Technology Co., Ltd. Beijing, China). Equal amounts of protein (10 μg) were separated by sodium dodecyl sulfate/polyacrylamide gel electrophoresis and transferred to a polyvinylidene fluoride membrane. The membrane was blocked in 5% nonfat dry milk for 4 h and probed with primary antibodies against TH (1:1000) and IBA-1 (1:1000) overnight at 4°C. After washing with TBST, the membranes were incubated for 1 h with a horseradish-peroxidase-conjugated anti-rabbit IgG (1: 2000). Protein bands were visualized using the enhanced ECL reagent and exposed on the X-ray film.

2.5 Behavioral tests

Rotarod test was carried out using an accelerating rotarod (ZH-300, Anhui

Zhenghua Biologic Apparatus Facilities Co. China) to study muscular coordination (Huang et al., 2017). Rats were tested at a set speed of 10 rpm/min, followed by an increase of 5 rpm/30 s, until the rats fell off the rungs. The cutoff time was 300 s. Rats were tested on Rotarod on day 40, 42, and 45 after ROT treatment.

Y maze test was performed for learning and memory. Successful alternation behavior was defined as entry into all three arms consecutively. The percentage of successful alternation was calculated as the ratio of the alternative to non-alternatives (Li et al., 2019).

The elevated plus maze test was one of the most widely used tests for measuring anxiety-like behavior. The test was based on the natural aversion of animals for open and elevated areas, as well as on their natural spontaneous exploratory behavior in novel environments. The apparatus consisted of open arms and closed arms, crossed in the middle perpendicularly to each other, and a center area (Li et al., 2019). The Y maze and elevated plus maze data were captured by a video monitor and analyzed using TopScan Lite 2.0 (CleverSys, Reston, VA, USA).

2.6 Bacterial DNA isolation

At the end of experiment, colon contents (150-200 mg) were collected in the lysis buffer (GSL) and stored at -80 °C until analysis. Bacterial DNA extraction was finished by TIANamp Stool DNA Kit. Briefly, bacteria in the lysis buffer were incubated for 10 min at 80°C to release DNA. After centrifugation, the supernatant (0.9 mL) was incubated with inhibit EX to absorb other materials. After centrifuge, the supernatant (200 μL) was mixed with 200 μL of GB buffer and protein kinase K, and incubated at 70 °C for 10 min. After adding 200 μL ethanol, the samples were applied to DNA column. After washing with GD and PW buffer, DNA was eluted in 50 μL TB buffer. The concentration of DNA was measured by Nanodrop (Nanodrop 1000, ThermoFisher, USA), and the purity

was assessed by 260/280 ratio (>1.9) and diluted to 20 ng/µL for real-time PCR analysis.

2.7 Real-time PCR analysis

The 15 µL PCR reaction mix contained 3 µL of bacterial DNA (20 ng/mL), 7.5 µL of iQ™ SYBR Green Supermix (Bio-Rad Laboratories, Hercules, CA), 0.5 µL of primer mix (10 µM each), and 4 µL of ddH_2O. After 5 min denature at 95°C, forty cycles were performed: annealing and extension at 60°C for 45 s and denature at 95°C for 10 s in CFX96 Touch™ Real-time PCR system (Bio-Rad Laboratories, Hercules, CA). Dissociation curve was performed after finishing 40 cycles to verify the quality of primers and amplification. The Ct values were used to calculate the expression of 16S rRNA genes by the $2^{-\Delta\Delta Ct}$ method and normalized to the total bacteria, and thus the expression of interested bacteria as relative transcript levels setting control as 100% as described (Medina et al., 2017; Wellman et al., 2017; Zhang et al., 2014; Uebanso et al., 2017). The primers were listed in **Table 1**.

2.8 Statistical Analysis

Data were indicated as mean ± standard error of the mean (SEM). Statistical significance was analyzed by one-way analysis of variance (ANOVA) or the nonpara-metric Mann–Whitney U test using GraphPad Prism software (GraphPad Software Inc., San Diego, CA, USA), as appropriate. Variations of statistical significance were further subjected to post hoc pairwise analysis by applying the Bonferroni's correction. A value of $p<0.05$ was considered statistically significant.

3. Results

3.1 Animal body weight and general health were observed

Four months after a single injection of LPS (5 mg/kg, i.p.), mice received

multi-injections of ROT (0.5 mg/kg, s.c., 5 week for 4 weeks). The dose of LPS and ROT were given far below the threshold dose in order to determine the low-grade neuroinflammation potentiating ROT-induced DA neurotoxicity (Huang et al., 2017; Li et al., 2019). The animal body weight was recorded weekly on the day of ROT injection and lasted for 45 days. All rats survived from ROT challenge. In general, as shown in **Figure 2**, no apparent changes in animal body weight were evident, except for body weight decrease in LR+HFD-removed group.

3.2 HFD attenuated LPS plus ROT-induced behavioral dysfunctions

Rats were tested on Rotarod on day 40, 42, and 45 after ROT treatment. As shown in **Figure 3A**, LPS plus ROT decreased the time rat stayed on rod by 25% and HFD-original, and HFD-reduced tended to increase the time, although not statistically significance was indicated. In the Y-maze test (**Figure 3B**), LPS plus ROT decreased the alteration rate by 28%, and HFD-original restored the correct alternation rate to 92% of Control group. In the elevated plus maze tests (**Figure 3C**), LPS plus ROT decreased the open arm activity nearly 50%, which was prevented by HFD-original treatment. Similar results were exhibited in the elevated plus maze (the Open arm/Close arm ratio) test (**Figure 3D**).

3.3 HFD protected DA neurons against LPS plus ROT-induced neurotoxicity

Loss of DA neurons in the SN was a main hallmarker in PD patients and PD animal models (Huang et al., 2017), which is associated with neuroinflammation in the area (Huang et al., 2017; Block et al., 2007). A single injection of LPS potentiated the neuroinflammation and DA neuronal loss in rats (Huang et al., 2017). As illustrated in **Figure 4A**, LPS plus ROT produced loss of DA neurons compared to control group (light green staining for TH positive neurons in the SN region). HFD-original restored DA neuronal loss

Journal Pre-proof

and HFD-reduced was also effective but produced less neuroprotection than HFD-original, while HFD-removed was ineffective.

To further confirm the immunofluorescence results, western blots analysis was performed to detect TH protein expression for DA neurons (**Figure 4B**). The expression of TH protein was decreased by 35% after LPS plus ROT administration compared to control group. HFD-original had better neuroprotection than HFD-reduced, whereas HFD-removed had no effects on LPS plus ROT-decreased TH protein expression.

3.4 HFD inhibited LPS plus ROT-induced microglial activation

Microglia-medicated neuroinflammation was involved in the pathogenesis of PD. Next, we investigated the effects of HFD on LPS plus ROT-induced microglial activation. As shown in **Figure 5A**, LPS plus ROT produced microglial activation compared to control group (light green staining with the protein of IBA-1). HFD-original decreased microglial activation and HFD-reduced was also effective but produced less anti-inflammation than HFD-original, while HFD-removed was ineffective. As shown in **Figure 5B**, the expression of IBA-1 protein was increased by 40% after LPS plus ROT treatment compared to control group. HFD-original and HFD-reduced attenuated microglial activation, whereas no significant inhibitory effects on microglia activation in HFD-removed group were indicated.

3.5 Gut microbiome alternations

At the end of the experiments, the colon content was collected and subjected to bacterial DNA extraction. The expressions of specific bacteria was determined using 16S rRNA probes. Results from 5 phyla, 9 families and 11 genus/species in a style of Phylum Family Probe using the total bacteria as internal controls were demonstrated. As shown in Figure 6, the increased bacteria by LPS plus ROT treatment was discerned. The increased bacteria

included phylum of *Verrucomicrobia, Bacteroidetes,* and *Firmicutes.* The mRNA expression of *Verrucomicrobia_Verrucomicrobaceae* (probe AJ400275 and AY271254) was markedly increased 7-8 fold by LPS plus ROT, which was attenuated by the treatment of HFD-original and HFD-reduced. The mRNA expression of *Bacteroidetes_Prevotellaceae_*(probe EU728784) was increased 2-fold by LPS plus ROT, and such an increase was prevented by HFD-original and HFD-reduced. The mRNA expression of *Firmutes_Lactobacillaceae* (probe KX247777) was also increased by LPS plus ROT by 60%, which was ameliorated by HFD-original and HFD-reduced. The mRNA expression of *Firmutes_Clostridaceae* (probe KU321269) was increased 70% by LPS plus ROT, but HFD treatments had no effects on its expression (**Figure 6A**). In addition, the decreased bacteria by LPS plus ROT was indicated. The mRNA expression of *Proteobacteria_Enterobactaceae* (probe Eco1457F and U02514) was decreased about 50% by LPS plus ROT. HFD-original increased it to the control levels. The mRNA expression of *Actinobacteria_Actinobacterias* (probe Act290F3) was decreased about 40% by LPS plus ROT, which was tended to increase in HFD-original and HFD-reduced groups. The mRNA expression of *Bacteroidetes_Porphymonadaceae* (probe KP07661) was decreased 60% by LPS plus ROT, and HFD did not affect its expression. The mRNA expression of *Bacteroidetes_Porphymonadaceae* (probe Provetella) was slightly reduced by LPS plus ROT, and no significant effects among HFD treatment groups were shown. The mRNA expression of *Firmutes_Firmicutes* (probe 926-1040 Firm) was slightly reduced by LPS plus ROT, and HFD tended to bring it to the control level (**Figure 6B**).

4. Discussion

The present study clearly demonstrated the protective effects of HFD against LPS plus ROT-induced DA neurotoxicity, as evidenced by the recused DA

neuronal loss, increased TH protein expression, and reduced microglial activation. HFD also improved behavioral dysfunctions via rotarod activity, Y maze and Elevated plus Maze tests. Furthermore, HFD was also effective in restoring LPS plus ROT-induced gut microbiota alterations. Furthermore, HFD-original produced more neuroprotection than HFD-reduced, while HFD-removed conferred no neuroprotection. These findings suggested that cinnabar and realgar were active ingredients in HFD. This study confirmed and extended our initial *in vitro* study using rat midbrain neuron-glia co-cultures (Zhang et al., 2012).

Microglia-mediated inflammatory responses are important events triggering the cascade of neurodegenerative diseases, such as PD (Block et al., 2007). A single injection of LPS induced chronic and low-grade neuroinflammation several months later (Qin et al., 2007; Huang et al., 2017; Li et al., 2019), which could aggravate neurodegeneration produced by a variety of neurotoxicants, including the pesticide ROT (Huang et al., 2017; Li et al., 2019), 1-methyl-4-phenyl-1, 2, 3, 6-tetrahydropyridine (MPTP) (Byler et al., 2009; Yu et al., 2013), α-synuclein (Zhang et al., 2016), and DSP-4 (N-(2-chloroethyl)-N-ethyl-2-bromobenzylamine), a selective noradrenergic neurotoxin (Jiang et al., 2015). Data from LPS plus ROT showed extensive proliferation of reactive microglia and increased levels of cytokines, such as TNFα, IL-1β, NO and PGE_2 in the SN (Huang et al., 2017), indicating neuroinflammation was the major contributor to DA neurodegeneration in LPS plus ROT-induced PD model. In this current study, HFD-original exerted more neuroprotection than HFD-reduced against LPS plus ROT-induced DA neurotoxicity and neuroinflammation, whereas HFD-removed had no neuroprotection. Consistent with the present study, our previous *in vitro* studies also found that HFD-original attenuated LPS-induced neuroinflammation and DA neuronal loss. However, HFD-reduced had the decreased efficacy and HFD-removed failed to protect against LPS-induced

neurotoxicity (Zhang et al., 2012; Zhang et al., 2010). These results demonstrated the importance of including cinnabar and realgar in this recipe.

The stages of PD brain pathology indicate that PD could start from the gut (Braak et al., 2003). The well-known neurotoxicants, such as ROT (Johnson et al., 2018; Yang et al., 2018) and MPTP (Perezpardo et al., 2018; Lai et al., 2018; Sun et al., 2018), produced profound effects on gut microbiota. Although microbiome sequencing is the main technique in gut microbiota analysis, real-time PCR with specific primers has also been performed to examine changes in microbiota, such as in the studies with ROT (Johnson et al., 2018), intestinal inflammation (Wellman et al., 2017), dietary Xylitol (Uebanso et al., 2017), short chain fatty acids (Unger et al., 2016), and antibiotics (Zhang et al., 2014), justifying the use of qPCR in the current approaches. Upon various bacteria in gut, *Verrucomicrobia* contains only a few described species. *Verrucomicrobia* are Gram-negative, coccoid or rod-shaped bacteria with unusual cellular structure, featuring wart-like cellular protrusions and a unique compartmentalized cell plan. *Verrucomicrobia* species have also been identified in human gastrointestinal tract. Increased *Verrucomicrobiaceae* are reported in PD patients from Finland (Scheperjans et al., 2015), Germany (Unger et al., 2016), and USA (Hill-Burns et al., 2017). In the present studies, LPS plus ROT increased *Verrucomicrobiaceae* 7-8 fold with two PCR probes, which was dramatically decreased by HFD-original and HFD-reduced treatments shown in Figure 6. In addition, *Lactobacillaceae* is a family of *Firmicutes*. In ROT-induced PD model, *Firmicutes* was increased, while *Bacteroidetes* was decreased, with much higher *Firmicutes/Bacteroidetes* ratio (Yang et al., 2018). Two of *Firmicutes* phylum probes (*Lactobacillaceae* and *Ruminoococaceae*) presented increases after LPS plus ROT. HFD-original was effective in decreasing LPS plus ROT-elevated *Lactobacillaceae.* Moreover, *Enterobacteriaceae* is a family of *Proteobacteria.* In PD animal models, Two of *Enterobacteriaceae* probes (Eco1457 and U02514) showed

decreases after LPS plus ROT treatment. HFD-original was effective in increasing LPS plus ROT reduced expression of *Enterobacteriaceae.* However, it should be noted that the examination of gut microbiome is dependent on the PCR probes. For example, there are two probes for *Provetalla* used in the present study, one probe (EU728784) showed increases by LPS plus ROT, while another probe (Provetella) showed a slight decrease. Thus, caution should be taken for interpreting the PCR data from microbiota as millions of bacteria exist and were diversified.

Cinnabar and realgar are frequently included in many traditional medicines, such as HFD. Similarly, many traditional medicines (Indian Ayurveda, Tibetan medicines and Chinese medicine) contain trace minerals to assist their therapeutic effects (Liu et al., 2018; Liu et al., 2019). The sulfide form of HgS and As_4S_4 are the major determinant of their disposition, therapeutic effects and the toxicity (Liu et al., 2019). Furtherly, the herbal mixtures can reduce the toxicity of cinnabar and realgar as exampled by An-Gong-Niu-Huang Wan (Xia et al., 2018). Additionally, cinnabar (HgS) and realgar (As_4S_4) are toxic heavy metal/metalloids, and the risk assessment frequently taken them as $HgCl_2$ and $NaAs_2O_3$ (Liu et al., 2018; Liu et al., 2008a; Liu et al., 2008b). At the clinical doses, HFD is much less toxic acutely as HgS and As_4S_4 to mice (Yan et al., 2011), or chronically toxic to rats (Peng et al., 2012). When rats were given orally HFD-original with 10% cinnabar and 10% realgar at the dose of 1.0 g/kg and 1/10 Hg as $HgCl_2$ for 10 days, HFD produced much less kidney Hg accumulation and renal injury as compared to $HgCl_2$ at 1/10 the of HFD Hg doses. $HgCl_2$ produced 25-fold induction of kidney injury molecule-1 (Kim-1), significantly decreased the expression of uptake transporter Oat1 and Oct2, and increased efflux transporter Mrp4 and Mate2K. All these changes were mild or absent in rats treated with HFD at 10-fold higher doses. However, there was no difference in toxicity with HFD-reduced (3% cinnabar and 3% realgar) and HFD-removed (without cinnabar and

realgar), suggesting that the toxic potential of HFD could not be evaluated based on $HgCl_2$. The effects of cinnabar (α-HgS) and Zuotai (β-HgS) on gut microbiota are also quite different from HgCl2 and methylmercury (Zhang et al., 2019).

It should be mentioned that patients taking HgS (both α-HgS and β-HgS)-containing traditional medicines, such as HFD, An-Gong-Niu-Huang Wan and Danzuo, there were no reported apparent toxic effects in the literature, and the side effects were also reversible after termination of medication (Ying et al., 2013; Sallon et al., 2017; Vickers et al., 2001; Li et al., 2014), fortifying the safe use of these traditional medicines according to the instructions of physicians.

In summary, the present study showed that (1) cinnabar-and realgar-containing HFD is effective in protecting against LPS plus ROT-induced neurotoxicity, and (2) the protection by HFD could be due, at least in part, to their beneficial effects on gut microbiota, and (3) removal of cinnabar and realgar from HFD recipe was ineffective, fortifying the scientific evaluation of metal-containing traditional remedies was needed.

Journal Pre-proof

Acknowledgements

This study was supported by the National Natural Science Foundation of China (No. 81760658), the foundation for High-level Innovative Talents of Guizhou Province (No. 20164027), Shijingshan's Tutor Studio of Pharmacology (No. GZS-201607), the Innovation Research Group project of Education Department of Guizhou Province (No. 2016038), the foundation for Excellent Young Talents of Zunyi Medical University (No.201603)

Author contributions

Jie Liu and Feng Zhang conceptualized the experiment. Ce Chen performed fluorescence staining of brain sections. An-Lin Hu and Ce Chen performed

behavioral tests. An-Lin Hu and Bin-Bin Zhang performed animal experiments and gut microbiome analysis. Ce Chen, Feng Zhang and Jie Liu wrote the manuscript. All authors reviewed and approved the final version of the manuscript. Feng Zhang and Jie Liu were the co-corresponding authors.

Conflict of interest statement

All authors declared no conflict of interest.

References

1. Block, M.L., Zecca, L., Hong, J.S..2007. Microglia-mediated neurotoxicity: uncovering the molecular mechanisms. Nature Reviews Neuroscience 8, 57-69.
2. Braak, H., Tredici, K. D., Rub, U., De Vos, R. A., Steur, E. N., Braak, E., 2003. Staging of brain pathology related to sporadic Parkinson's disease. Neurobiology of Aging 24, 197-211.
3. Byler, S. L., Boehm, G. W., Karp, J. D., Kohman, R. A., Tarr, A. J., Schallert, T., 2009. Systemic lipopolysaccharide plus MPTP as a model of dopamine loss and gait instability in C57Bl/6J mice. Behavioural Brain Research 198, 0-439.
4. Dodiya, H. B., Forsyth, C. B., Voigt, R. M., Engen, P. A., Patel, J., Shaikh, M., Green, S.J., Naqib, A., Roy, A., Kordowerd, J.H., Pahan, K., Shannon, K.M., Keshavarzian, A., 2018. Chronic stress-induced gut dysfunction exacerbates Parkinson's disease phenotype and pathology in a rotenone-induced mouse model of Parkinson's disease. Neurobiology of disease.
5. Galland, L., 2014. The gut microbiome and the brain. Journal of medicinal food 17, 1261-1272.
6. Hill‐Burns, E. M., Debelius, J. W., Morton, J. T., Wissemann, W. T., Lewis, M. R., Wallen, Z. D., Knight, R. Peddada, S.D., Factor, S.A., Molho, E.,

Zabetian, C.P., Knight, R., Payami, H., 2017. Parkinson's disease and Parkinson's disease medications have distinct signatures of the gut microbiome. Movement disorders 32, 739-749.

7. Huang, C., Zhu, L., Li, H., Shi, F., Wang, G., Wei, Y., Zhang, F., 2017. Adulthood Exposure to Lipopolysaccharide Exacerbates the Neurotoxic and Inflammatory Effects of Rotenone in the Substantia Nigra. Frontiers in Molecular Neuroscience 10,131.
8. Jiang, L., Chen, S. H., Chu, C. H., Wang, S. J., Oyarzabal, E., Wilson, B., Hong, J. S., 2015. A novel role of microglial NADPH oxidase in mediating extra‐synaptic function of norepinephrine in regulating brain immune homeostasis. Glia 63, 1057-1072.
9. Johnson, M. E., Stringer, A., Bobrovskaya, L. 2018. Rotenone induces gastrointestinal pathology and microbiota alterations in a rat model of Parkinson’s disease. Neurotoxicology 65, 174-185.
10. Lai, F., Jiang, R., Xie, W., Liu, X., Tang, Y., Xiao, H., Gao, J., Jia, Y., Bai, G., 2018. Intestinal pathology and gut microbiota alterations in a methyl-4-phenyl-1, 2, 3, 6-tetrahydropyridine (MPTP) mouse model of Parkinson’s disease. Neurochemical research 43, 1986-1999.
11. Li, C., Wang, D. P., Duo, J., Duojie, L. D., Chen, X. M., Du, Y. Z., Wei, L. X. 2014. Study on safety of Tibetan medicine zuotai and preliminary study on clinical safety of its compound dangzuo. Zhongguo Zhong yao za zhi= Zhongguo zhongyao zazhi= China journal of Chinese materia medica 39, 2573-2582.
12. Li, H., Song, S., Wang, Y., Huang, C., Zhang, F., Liu, J., Hong, J., 2019. Low-Grade Inflammation Aggravates Rotenone Neurotoxicity and Disrupts Circadian Clock Gene Expression in Rats. Neurotoxicity Research 35, 421-431.
13. Liu, J., Lu, Y., Wu, Q., Goyer, R. A., Waalkes, M. P., 2008a. Mineral Arsenicals in Traditional Medicines: Orpiment, Realgar, and Arsenolite.

Journal of Pharmacology and Experimental Therapeutics 326, 363-368.

14. Liu, J., Shi, J., Yu, L., Goyer, R. A., Waalkes, M. P., 2008b. Mercury in Traditional Medicines: Is Cinnabar Toxicologically Similar to Common Mercurials? Experimental Biology and Medicine 233, 810-817.
15. Liu, J., Wei, L., Wang, Q., Lu, Y., Zhang, F., Shi, J., Cherian, M. G., 2018. A review of cinnabar (HgS) and/or realgar (As4S4)-containing traditional medicines. Journal of Ethnopharmacology 340-350.
16. Liu, J., Zhang, F., Ravikanth, V., Olajide, O. A., Li, C., Wei, L., 2019. Chemical Compositions of Metals in Bhasmas and Tibetan Zuotai Are a Major Determinant of Their Therapeutic Effects and Toxicity. Evidence-based Complementary and Alternative Medicine. 2019:1697804
17. Martin, C. R., Osadchiy, V., Kalani, A., Mayer, E. A., 2018. The Brain-Gut-Microbiome Axis. Cellular and Molecular Gastroenterology and Hepatolog 6, 133-148.
18. Medina, D. A., Pedreros, J. P., Turiel, D., Quezada, N., Pimentel, F., Escalona, A., Garrido, D., 2017. Distinct patterns in the gut microbiota after surgical or medical therapy in obese patients. PeerJ 5, e3443.
19. Peng, F., Yang, H., Wu, Q., Liu, J., Shi, J., 2012. Studies on subacute toxicity of Wansheng Huafeng Dan in rats. Zhongguo Zhong Yao Za Zhi 37, 1017-1022.
20. Perezpardo, P., Dodiya, H. B., Engen, P., Naqib, A., Forsyth, C. B., Green, S. J., Kraneveld, A. D., 2018. Gut bacterial composition in a mouse model of Parkinson's disease. Beneficial Microbes 9, 799-814.
21. Pharmacopoeia, Pharmacopoeia of the People's Republic of China, Vol. 1. Chinese Medical Press 2015. 1.
22. Qin, L., Liu, Y., Hong, J. S., Crews, F. T., 2013. NADPH oxidase and aging drive microglial activation, oxidative stress and dopaminergic neurodegeneration following systemic LPS administration. Glia 61, 855-868.

23. Qin, L., Wu, X., Block, M. L., Liu, Y., Breese, G. R., Hong, J. S., Crews, F. T., 2007. Systemic LPS causes chronic neuroinflammation and progressive neurodegeneration. Glia 55, 453-462.
24. Radad, K., Hassanein, K., Moldzio, R., Rausch, W. D, 2013. Vascular damage mediates neuronal and non-neuronal pathology following short and long-term rotenone administration in Sprague-Dawley rats. Experimental and toxicologic pathology 65, 41-47.
25. Sallon, S., Dory, Y., Barghouthy, Y., Tamdin, T., Sangmo, R., Tashi, J., Bdolahabram, T., 2017. Is mercury in Tibetan Medicine toxic? Clinical, neurocognitive and biochemical results of an initial cross-sectional study. Experimental Biology and Medicine 242, 316-332.
26. Scheperjans, F., Aho, B. A., Pereira, P., Koskinen, K., Paulin, L., Pekkonen, E., Auvinen, P., 2015. Gut microbiota are related to Parkinson's disease and clinical phenotype. Movement disorders 30, 350-358.
27. Spielman, L. J., Gibson, D. L., Klegeris, A., 2018. Unhealthy gut, unhealthy brain: The role of the intestinal microbiota in neurodegenerative diseases. Neurochemistry International 120, 149-163.
28. Sun, M. F., Zhu, Y. L., Zhou, Z. L., Jia, X. B., Xu, Y. D., Yang, Q., 2018. Neuroprotective effects of fecal microbiota transplantation on MPTP-induced parkinson’s disease mice: gut microbiota, glial reaction and TLR4/TNF-α signaling pathway. Brain Behavior and Immunity 70, 48-60.
29. Uebanso, T., Kano, S., Yoshimoto, A., Naito, C., Shimohata, T., Mawatari, K., Takahashi, A., 2017. Effects of Consuming Xylitol on Gut Microbiota and Lipid Metabolism in Mice. Nutrients 9, E756.
30. Unger, M. M., Spiegel, J., Dillmann, K., Grundmann, D., Philippeit, H., Burmann, J., Schafer, K., 2016. Short chain fatty acids and gut microbiota differ between patients with Parkinson's disease and age-matched controls. Parkinsonism & Related Disorders 32, 66-72.
31. Vickers, A. J., Van Haselen, R., Heger, M., 2001. Can Homeopathically

Prepared Mercury Cause Symptoms in Healthy Volunteers? A Randomized, Double-Blind Placebo-Controlled Trial. Journal of Alternative and Complementary Medicine 7, 141-148.

32. Wang, Y., Wang, Z., Wang, Y., Li, F., Jia, J., Song, X., Wang, Y., 2018. The Gut-Microglia Connection: Implications for Central Nervous System Diseases. Frontiers in Immunology 9, 2325.
33. Wellman, A. S., Metukuri, M. R., Kazgan, N., Xu, X., Xu, Q., Ren, N. S., Li, X., 2017. Intestinal Epithelial Sirtuin 1 Regulates Intestinal Inflammation during Aging in Mice by Altering the Intestinal Microbiota. Gastroenterology 153, 772-786.
34. Xia, F., Li, A., Chai, Y., Xiao, X., Wan, J., Li, P., Wang, Y. 2018. UPLC/Q-TOFMS-Based Metabolomics Approach to Reveal the Protective Role of Other Herbs in An-Gong-Niu-Huang Wan Against the Hepatorenal Toxicity of Cinnabar and Realgar. Frontiers in pharmacology 9.
35. Yang, X., Qian, Y., Xu, S., Song, Y., Xiao, Q., 2018. Longitudinal Analysis of Fecal Microbiome and Pathologic Processes in a Rotenone Induced Mice Model of Parkinson's Disease. Frontiers in Aging Neuroscience 9, 441.
36. Yan, J.W., Miao, J.W., He, H.Y., Shi, J.Z., Wu, Q., Liu, J., Shi, J.S., 2011. Hua-Feng-Dan differs from realgar and cinnabar in producing acute toxicity to the liver and kidney of mice. Zhongguo Yaoli Duli Zazhi 4, 380-385.
37. Ying, S. 2013. Progress in Pharmacological and Clinical Research of Qishiwei Zhenzhu Wan. Chinese Journal of Experimental Traditional Medical Formulae 19, 367-371.
38. Yu, L., Wei, H. L., Bao, X., Zhang, D., Sun, H., 2013. Therapeutic effect of a natural squamosamide derivative FLZ on Parkinson's disease model mice induced by LPS plus MPTP. Yao Xue Xue Bao 48, 1557-1562.
39. Zhang, B.B., Liu, Y.M., Hu, A.L., Xu, S.F., Fan, L.D., Chang, M.L., Li, C., Wei, L.X., Liu, J., 2019. HgS and Zuotai differ from HgCl2 and methyl mercury in intestinal Hg absorption, transporter expression and gut

microbiome in mice. Toxicology and Applied Pharmacology.

40. Zhang, F., Lu, Y., Liu, J., Shi, J., 2010. Realgar is active ingredient of Angong Niuhuang pill in protection against LPS-induced neuroinflammation. Zhongguo Zhong Yao Za Zhi 35, 3333-3338.
41. Zhang, F., Lu, Y., Wu, Q., Yan, J., Shi, J., Liu, J., 2012. Role of cinnabar and realgar of WSHFD in protecting against LPS-induced neurotoxicity. Journal of Ethnopharmacology 139, 822-828.
42. Zhang, W., Gao, J. H., Yan, Z. F., Huang, X. Y., Guo, P., Sun, L., 2016. Minimally toxic dose of lipopolysaccharide and α-synuclein oligomer elicit synergistic dopaminergic neurodegeneration: role and mechanism of microglial nox2 activation. Molecular Neurobiology 55, 1-14.
43. Zhang, Y., Limaye, P. B., Renaud, H. J., Klaassen, C. D., 2014. Effect of various antibiotics on modulation of intestinal microbiota and bile acid profile in mice. Toxicology and Applied Pharmacology 277, 138-145.
44. Zhou, X., Wang, Q., Yang, X., 2009. Progresses on mechanisms of pharmacological and toxicological effects of cinnabar. Zhongguo Zhong Yao Za Zhi 34, 2843-2847.

Journal Pre-proof

Journal Pre-proof

Table 1. Primer sequences for PCR.

Phylum	Family	Gene access #	Forward	Reverse
Verrucomicrobia	Verrucomicrobiaceae	AJ400275	ATCATTCACAATGGGGGAAA	GGCACAGAGTTAGCCGTCTC
		AY271254	ATCATTCACAATGGGGGAAA	GGCACAGAGTTAGCCGTCTC
Bacteroidetes	Prevotellaceae	EU728784	CGAAAGGTTTAGCGGTGAAG	CGTAGGAGTTTGGACCGTGT
	Bacteroidaceae	Prevotella	GGTGTCGGCTTAAGTGCCAT	CGGACGTAAGGGCCGTGC
	Porphymonadaceae	KP07661	ACACGGACCAGACTCCTACG	ACACGTCCCGCACTTTATTC
Actinobacteria	Actinobacterias	Act290F3	TACGGCCGCAGGCTA	TCRTCCCCACCTTCCTCCG
Firmicutues	Firmitutes	926-1040 Firm	GGAGYATGTGGTTTAATTCGAAGCA	AGCTGACGACAACCATGCAC
	Lactobacillaceae	KX247777	TTTGAGTGAGTGGCGAACTG	CCAAAAGTGATAGCCGAAGC
	Clostridaceae	KU321269	ATATTGCACAATGGGGGAAA	AGCCGGAGCTTTCTCCTTAG
Proteobacteria	Enterobacteriaceae	Eco1457F	CATTGACGTTACCCGCAGAAGAAGC	CTCTACGAGACTCAAGCTTGC
	Enterobacteriaceae	U02514	GATTGTCGCTCTTCCAGCTC	GTCCGCAACCGTTGAGTAAT
Total Bacteria		Eub338-518	ACT CCT ACG GGA GGC AGC AG	ATTACCGCGGCTGCTGG
Universal Bacteria		Universal	TCCTACGGGAGGCAGCAGT	GGACTACCAGGGTATCTAATCCTGTT

Journal Pre-proof

Figure Legends

Figure 1. Experimental design.

Figure 2. Animal body weight was shown. Rats were given a single injection of LPS (5 mg/kg, i.p.), and 4 months later challenged with ROT (0.5 mg/kg, s.c., 5/week for 4 weeks). HFD (0.6 g/kg), including HFD-removed (without cinnabar and realgar), HFD-reduced (containing 3% cinnabar and 3% realgar) and HFD-original (containing 10% cinnabar and 10% realgar) were given via feed for 46 days starting from ROT administration. All data were from the one-way ANOVA analysis. Data were mean ± SEM from 6 rats.

Figure 3. HFD attenuated LPS plus ROT-induced behavioral dysfunctions. Rotarod test (A), Y-maze test (B), Elevated Plus Maze test with activity at the open arm (C) and the ratio of Open arm/Close arm activities (D) were evaluated. All data were from the one-way ANOVA analysis. Data were mean ± SEM from 6 rats. $^{*}p<0.05$ compared with the control group; $^{\#}p< 0.05$ compared with LPS plus ROT group.

Figure 4. HFD protected DA neurons against LPS plus ROT-induced neurotoxicity. DA neuronal lesion in SN was analyzed via the DA neuronal counting by immunofluorescence staining with an anti-TH antibody (A). The “ellipse” presented the area of SN. Scale bar = 200 μm. TH protein expression was detected by western blot assay (B). All data were from the one-way ANOVA analysis. Data were mean ± SEM from 6 rats. $^{*}p<0.05$ compared with the control group; $^{\#}p< 0.05$ compared with LPS plus ROT group; $^{\&}p< 0.05$ compared with LR+HFD-reduced group.

Figure 5. HFD inhibited LPS plus ROT-induced microglial activation. Microglial activation was analyzed by immunofluorescence staining with an

anti-IBA-1 antibody and the number of positive IBA-1 cells was counted (A). Scale bar = 100 μm. IBA-1 protein expression was detected by western blot assay (B). All data were from the one-way ANOVA analysis. Data were mean ± SEM from 6 rats. $^{*}p<0.05$ compared with the control group; $^{\#}p<0.05$ compared with LPS plus ROT group; $^{\&}p<0.05$ compared with LR+HFD-reduced group.

Figure 6. Gut microbiome of the mRNA expressions after LPS plus ROT-induced DA neuronal damage was analyzed. The mRNA expressions of phylum of Verrucomicrobia, phylum of Proteobacteria, Actinobacteria, Bacteroidetes and Firmicutes were detected by real-time PCR. All data were from the Mann–Whitney U test. Data were mean ± SEM from 6 rats. $^{*}p<0.05$ compared with the control group; $^{\#}p< 0.05$ compared with LPS plus ROT group.

Journal Pre-proof

Figure 1

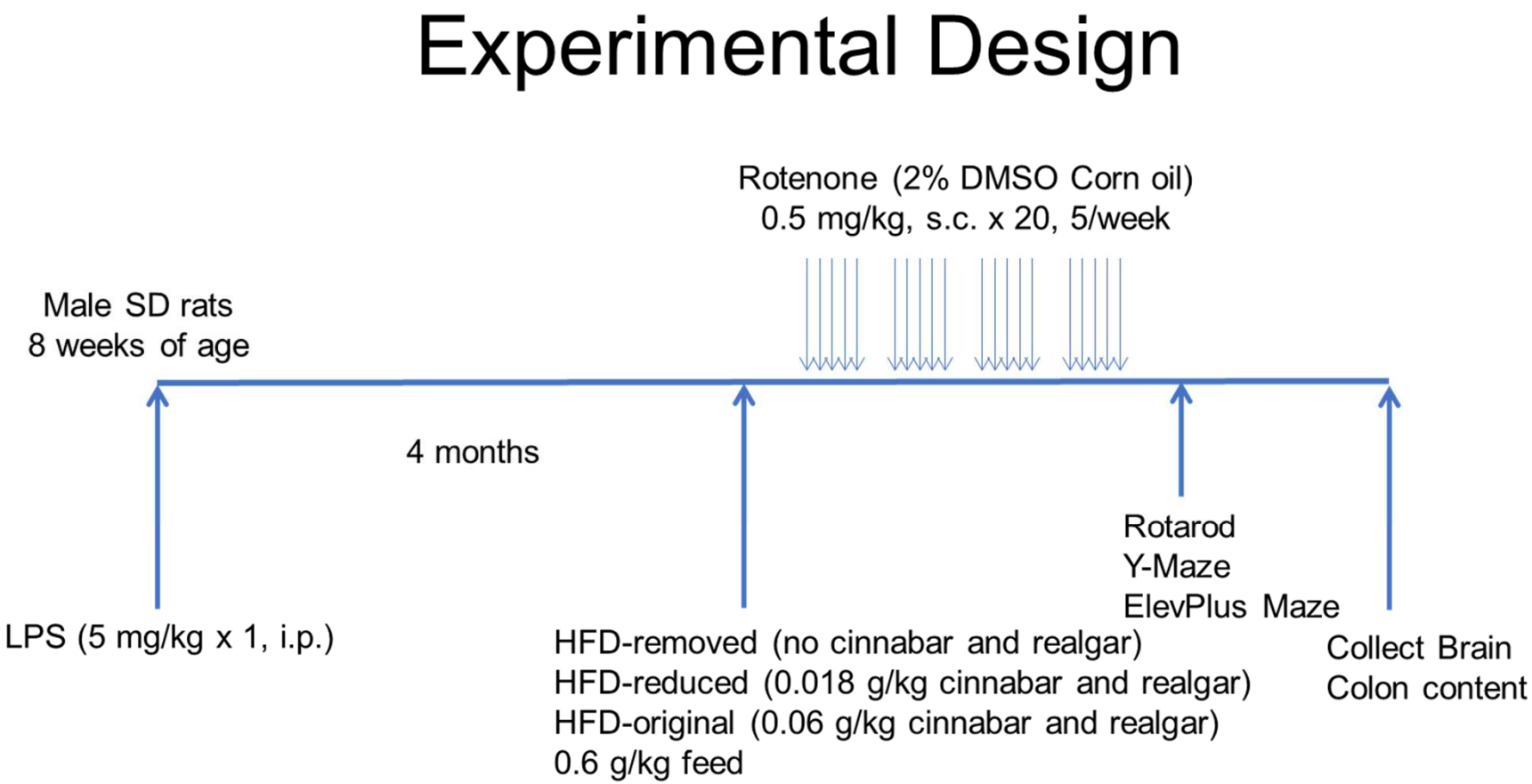
Experimental Design
Rotenone (2% DMSO Corn oil)
0.5 mg/kg, s.c. x 20, 5/week
Male SD rats
8 weeks of age
4 months
Rotarod
Y-Maze
ElevPlus Maze
LPS (5 mg/kg x 1, i.p.)
HFD-removed (no cinnabar and realgar)
HFD-reduced (0.018 g/kg cinnabar and realgar)
HFD-original (0.06 g/kg cinnabar and realgar)
0.6 g/kg feed
Collect Brain
Colon content

Figure 2

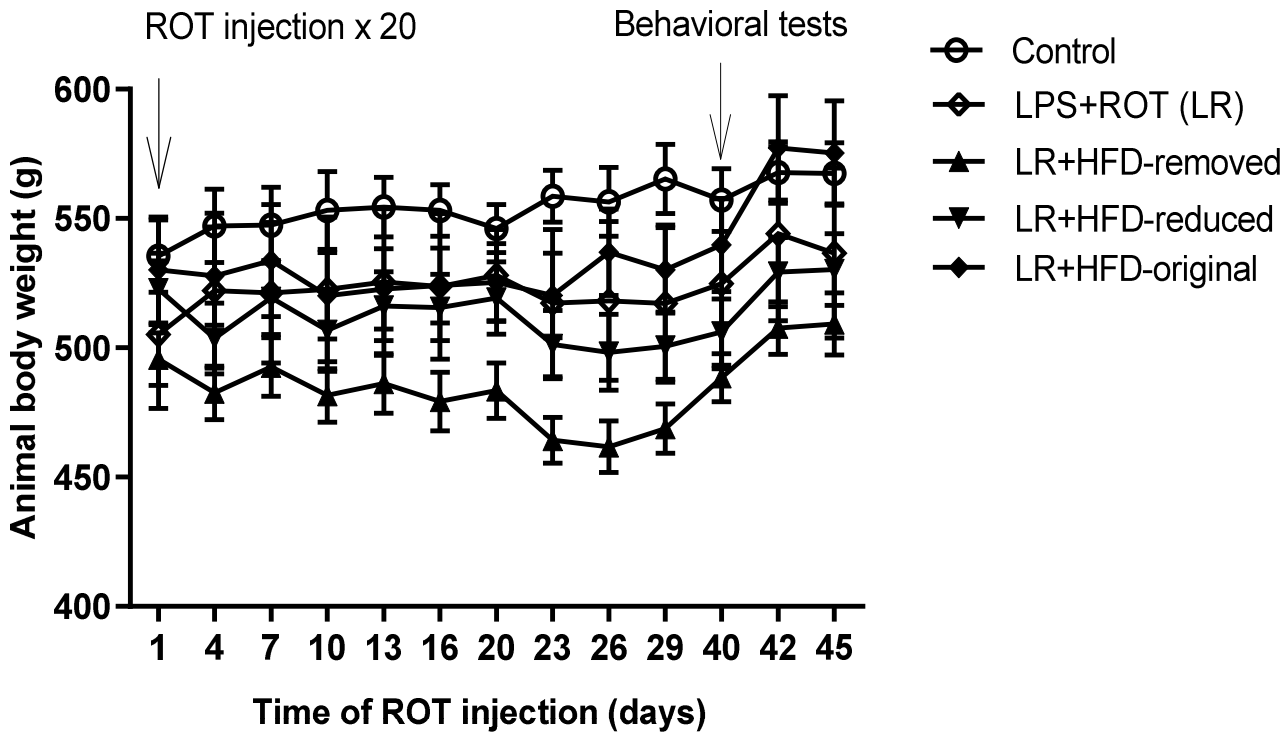
ROT injection x 20
Behavioral tests
Animal body weight (g)
600
550
500
450
400
1
4
7
10
13
16
20
23
26
29
40
42
45
Time of ROT injection (days)
Control
LPS+ROT (LR)
LR+HFD-removed
LR+HFD-reduced
LR+HFD-original

Figure 3

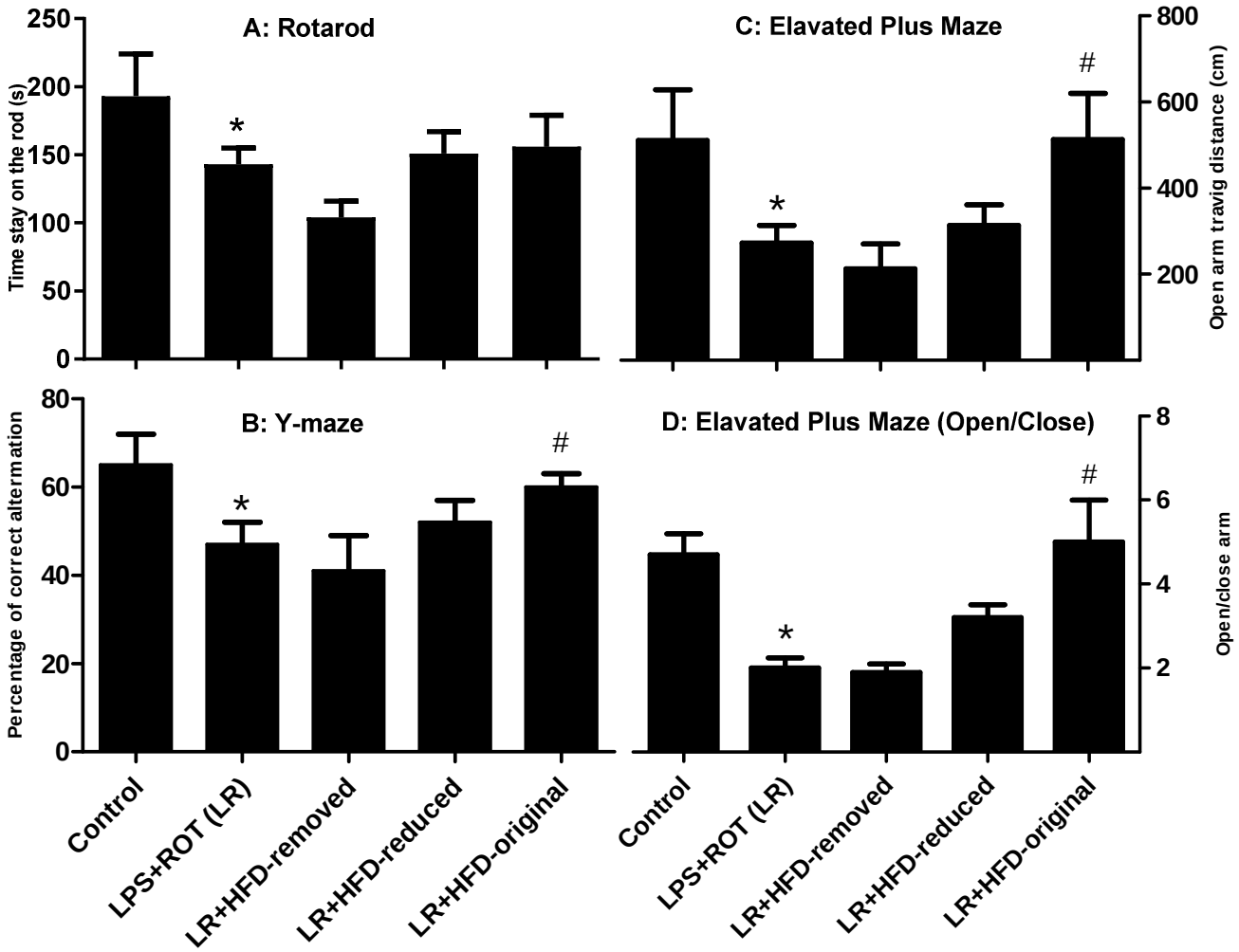
A: Rotarod
Time stay on the rod (s)
250
200
150
100
50
0
C: Elavated Plus Maze
Open arm travig distance (cm)
800
600
400
200
B: Y-maze
Percentage of correct alternation
80
60
40
20
0
D: Elavated Plus Maze (Open/Close)
Open/close arm
8
6
4
2
*
#
Control
LPS+ROT (LR)
LR+HFD-removed
LR+HFD-reduced
LR+HFD-original

Figure 4

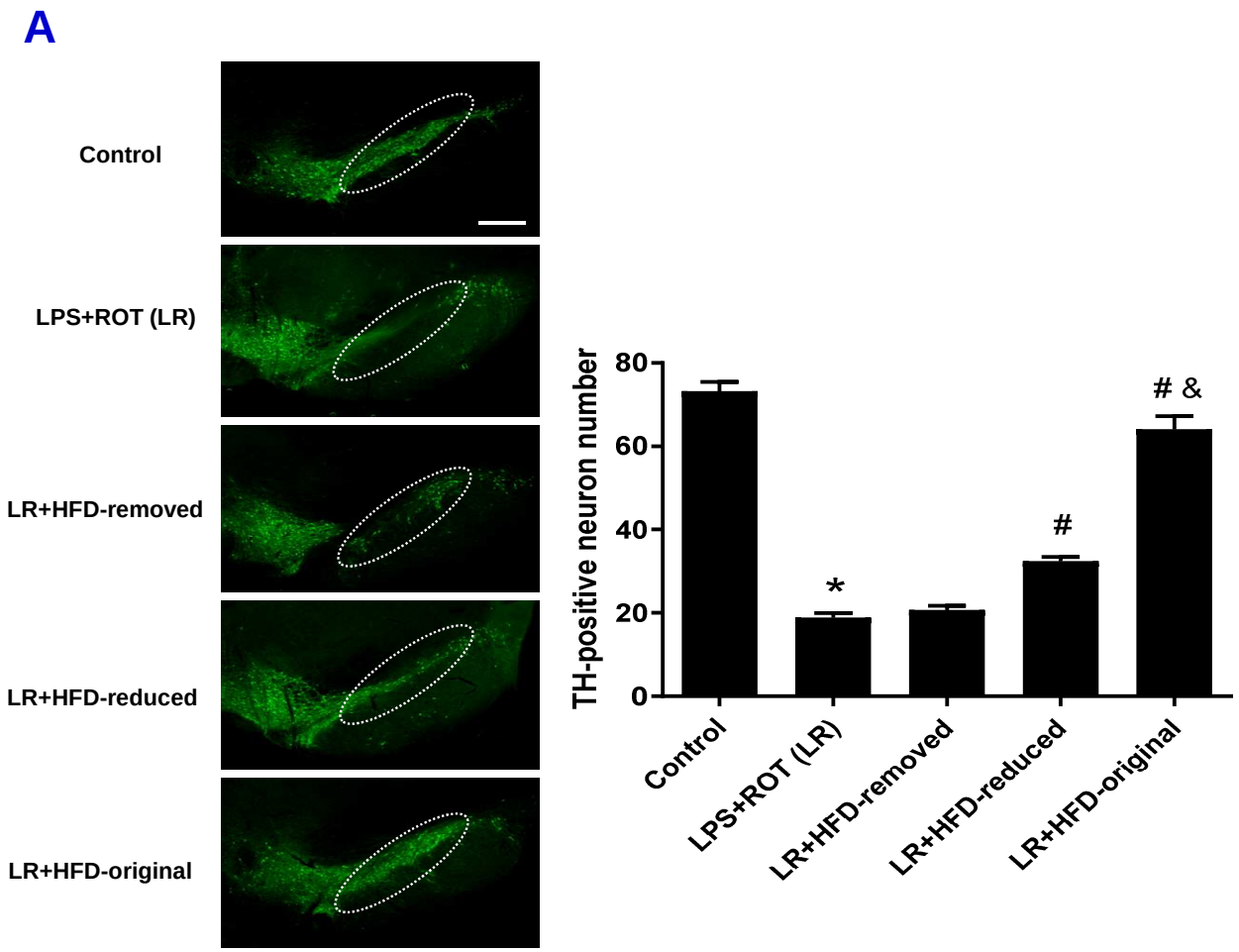
A
Control
LPS+ROT (LR)
LR+HFD-removed
LR+HFD-reduced
LR+HFD-original
TH-positive neuron number
80
60
40
20
0
*
#
&
Control
LPS+ROT (LR)
LR+HFD-removed
LR+HFD-reduced
LR+HFD-original
B
LPS - + + + +
ROT - + + + +
HFD - - - 3% 10%
TH
β-actin
TH/β-actin (% of control)
150
100
50
0
*
#
&
Control
LPS+ROT (LR)
LR+HFD-removed
LR+HFD-reduced
LR+HFD-original

Figure 5

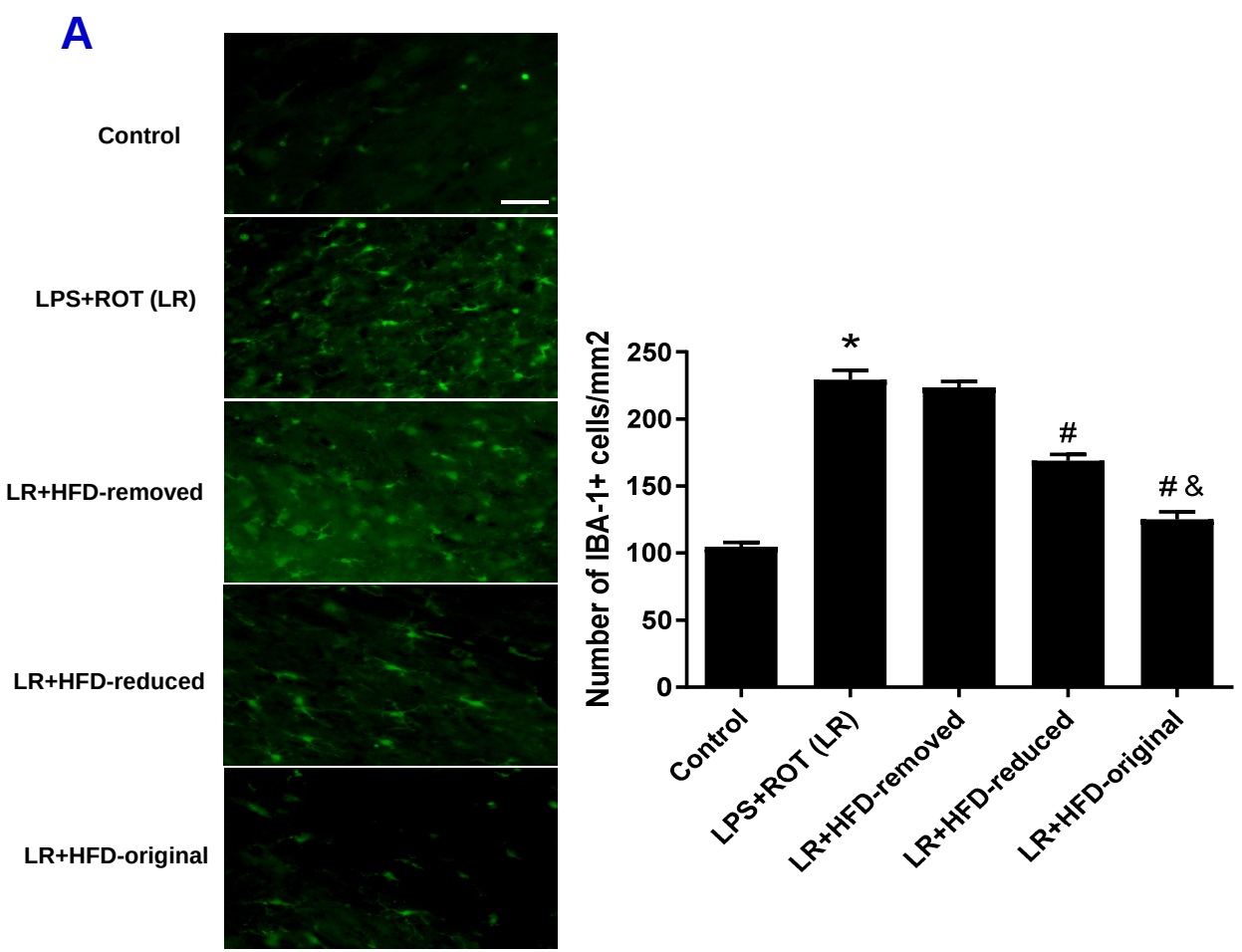
A
Control
LPS+ROT (LR)
LR+HFD-removed
LR+HFD-reduced
LR+HFD-original
Number of IBA-1+ cells/mm2
250
200
150
100
50
0
*
#
&
Control
LPS+ROT (LR)
LR+HFD-removed
LR+HFD-reduced
LR+HFD-original

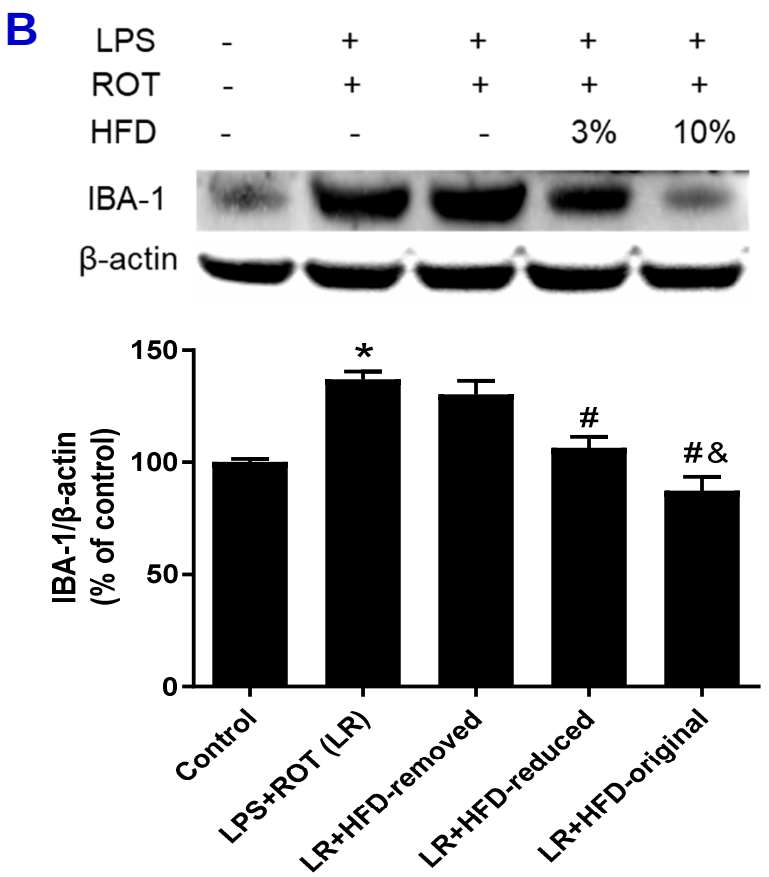
B
LPS - + + + +
ROT - + + + +
HFD - - - 3% 10%
IBA-1
β-actin
IBA-1/β-actin
(% of control)
150
100
50
0
*
#
&
Control
LPS+ROT (LR)
LR+HFD-removed
LR+HFD-reduced
LR+HFD-original

Figure 6

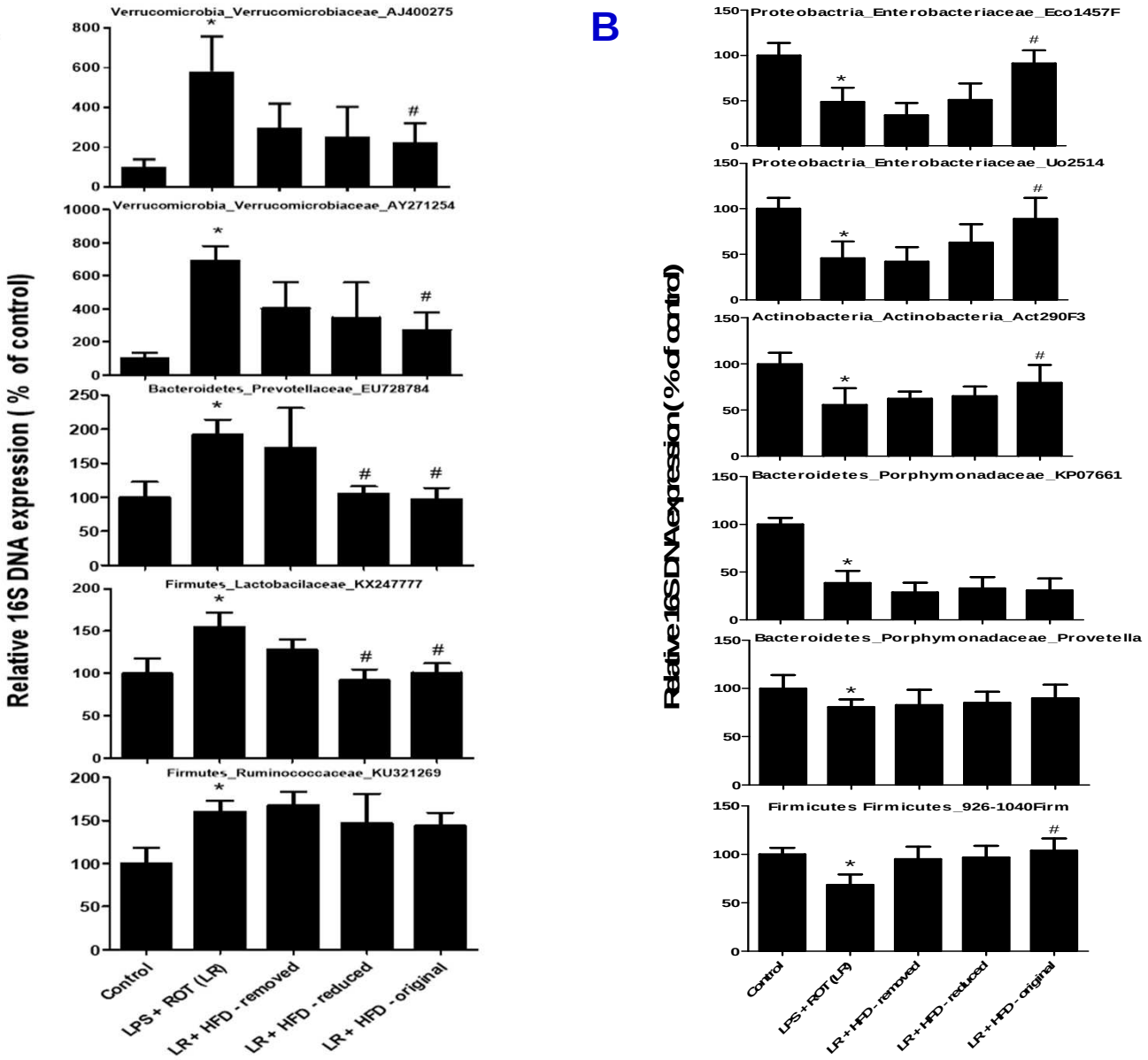
A
Verrucomicrobia_Verrucomicrobiaceae_AJ400275
Verrucomicrobia_Verrucomicrobiaceae_AY271254
Bacteroidetes_Prevotellaceae_EU728784
Firmutes_Lactobacilaceae_KX247777
Firmutes_Ruminococcaceae_KU321269
Relative 16S DNA expression (% of control)
Control
LPS + ROT (LR)
LR + HFD - removed
LR + HFD - reduced
LR + HFD - original
B
Proteobactria_Enterobacteriaceae_Eco1457F
Proteobactria_Enterobacteriaceae_Uo2514
Actinobacteria_Actinobacteria_Act290F3
Bacteroidetes_Porphymonadaceae_KP07661
Bacteroidetes_Porphymonadaceae_Provetella
Firmicutes Firmicutes_926-1040Firm
Relative 16S DNA expression (% of control)
Control
LPS + ROT (LR)
LR + HFD - removed
LR + HFD - reduced
LR + HFD - original